Bulgarian Chemical Communications, Volume 51, Special Issue F (pp. 5 - 10) 2019

Research of specific destruction energy of the porous coatings at power units

A. A. Genbach[1], K. K. Shokolakov[1], D. Yu. Bondartsev[1], I. K. Iliev[2*], A. K. Terziev[3]

[1] *Almaty University of Energy and Communications, Faculty of Heat & Power Units*
[2]*University of Ruse, Dept. of Thermal Engineering, Hydraulics and Ecology, 8 Studentska str., 7017 Ruse, Bulgaria,*
3 Technical University of Sofia, Dept. of Power Engineering and Power Machines,8 Kliment Ohridski blvd., 1000 Sofia, Bulgaria

Methods and devices of the capillary porous system were developed for the turbine equipment of power plants. The scientific methodology of their research was established and study was carried out for the limit heat flows at metal and poor conductive porous structures as granite coatings working under joint action of gravity and capillary forces. Mathematical model is based on the thermoelasticity problem. Mechanism of the destruction process for analogy of heat exchange of poor conductive coatings of minor porosity and metal base was also described. The revealed values of specific destruction energy allow extending the critical cases in the porous system of cooling and ensuring the most suitable choice of porous coatings of minor porosity and heat conductivity.

Keywords: heat exchange, porous structure, heat power plants

INTRODUCTION

The main problem determining the development of the energy industry is the problem of uneconomic production and use of energy. One of the ways to reduce losses from external irreversibility of thermal processes in gas turbine plants is to reduce the temperature between the media. The main tendency emerging at the present stage of development of both domestic and foreign stationary gas turbine unit (GTU) is the increase of initial gas parameters before the turbine – it is this tendency that determines the steady growth of efficiency of newly designed powerful GTUs.

Application of porous materials in the steam turbine equipment has motivated many researches to develop new devices. The intensity of heat discharging systems and boosting of processes [1-2] inside them was observed. Application of porous materials apart from cooling systems help to develop devices and solve problems of explosion safety, health and durability [3-4]. It was possible to control processes of steam generation due to the excessive liquid in porous and capillary structures formed by capillary and mass forces [1-4].

At heat and power units (HPU) capillary porous materials are used for cooling highly boosted detonation burners [1], forming steam coolers in steam boilers [3], oil coolers that avoid oil and water penetration into the cooling water and bearing system, labyrinth sealing, and other devices [4].

Previously, using the methods of photoelasticity and holography, the destruction mechanism of the porous cooling system of the fire-jet burners' combustion chambers and nozzles was investigated [1]. It is interesting to compare the intensity of heat transfer [5-7] and the surface limit state [8, 9, 12], as well as to evaluate possible mechanisms for the destruction of heating surfaces covered with capillary-porous structures [1-4]. This is in relation to the tasks of increasing the capacity of the thermal power equipment of power plants [10, 11]. Such a problem is long overdue in connection with the modernization and extension of the life of gas turbine power plants.

EXPERIMENTAL STUDY

The process of destruction of capillary-porous coatings of granite, quartz and tesenite is investigated. Coatings were applied to a heat exchange surface (metal wall) with a gas flame rocket burner at a temperature of 2500 ÷ 3000 °C and a flow velocity of 2000 m/s, using a fine fraction (husk). It was obtained by treating rocks with a rocket-type burner. The porosity of the coatings was (3÷30) %. Their destruction was carried out using the torch of a thermoset burner (Fig.1).

The burner, combustion chamber and nozzle were protected by porous coatings (they simulate similar devices of gas turbines). For measurement of the heat flux, a heat receiver was used,

* To whom all correspondence should be sent:
iiliev@enconservices.com

consisting of a copper cylinder, which perceived the action of a gas jet from one end, and was cooled by water from the other.

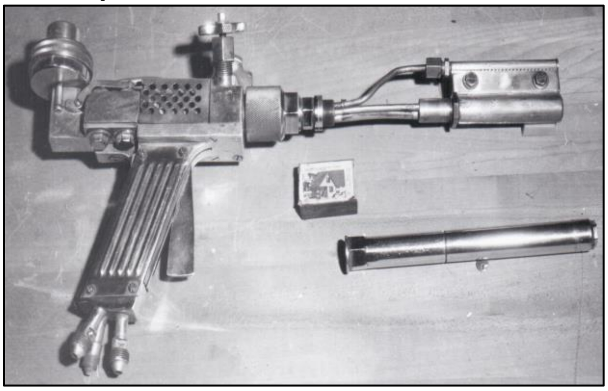

Fig.1. General view of the experimental plant in the form of a rocket flame-jet rocket burner torch

Ceramic made of zirconium dioxide was used as an insulator. The chromel-kopel thermocouples were placed in a copper cylinder. The thermal balance mismatch did not exceed ± 12%, and the maximum relative error in determining qi did not exceed ± 7%. The coordinate device mounted on the burner made it possible to establish a stagnation spot (spreading) of the gas stream in the area of the temperature sensor.

The most difficult part of the experiment was the ability to determine of the size of the detached particles at the time of the limiting state of the coatings. To cope with the issue a filming method using the SKS-1M camera was used (Fig.2 and Fig.3).

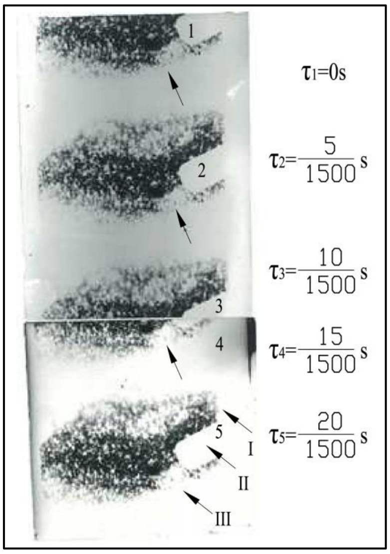

Fig.2. Record of the husk flight of size $\delta = 2{,}5 \cdot 10^3$ m at destruction of the granite coating particle by the rocket burner ($q = 1{,}2 \cdot 10^6$ W/m^2): I – capillary porous coating; II – trunk of burner where the supersonic high temperature pulse detonation gas flow comes from; III – particle pulled from coating

Refrigerant was supplied from the pressure tank under a slight overpressure $(0{,}2 \div 0{,}25) \cdot 10^5$Pa. Its consumption is reduced by $60 \div 70$ times, because heat removal is carried out by vaporization. Heat flow is transmitted through the walls of the chamber and the nozzle, the value of which varies widely (by one to two orders of magnitude).

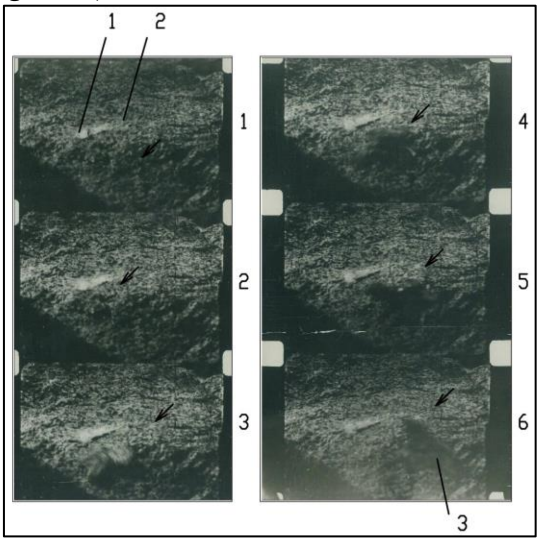

Fig.3. Fragment of a high-speed shooting of the destruction of a teshenite with a rocket flame-jet burner with a specific heat flux equal to $1{,}2 \cdot 10^6$ W/m^2. A shell with a size of $2{,}5 \cdot 10^{-3}$ forms for 2,2 s. A line of destruction of "equal possibilities" is clearly visible (arrow): 1 – capillary-porous coating; 2 – particle (shell) detached from the coating; 3 – line of destruction of "equal possibilities". Cinemagram of particle flight in time: τ_1 to τ_6: 1 = 0 s; 2 = 5/1500 s; 3 = 10/1500 s; 4 = 15/1500 s; 5 = 20/1500 s; 6 = 25/1500 s

It reaches the highest value in the zone of the critical section of the nozzle. However, the self-adaptive ability of the system successfully copes with this working mode and ensures uniform distribution of the temperature field in the cooled walls. Stagnation or formation of a vapour bubble in narrow cooling channels, leading to burnout of the walls, as is the case with a once-through cooling system, is eliminated. The requirements for sealing the connection of the combustion chamber with the distribution head of the burner are reduced.

SIMPLIFIED BURNER DESIGN AND OPERATION

The capillary - porous structure is removable, for which it is enough to unscrew it from the distribution head together with the combustion chamber. In a detached form, the structure can be cleaned from mechanical and chemical deposits and again easily installed on the burner, i.e. repeatedly restored with a minimum investment in time (several minutes). A very low water flow rate, for example (3 ÷ 4)·10^{-3} kg / s for a TR-14/22 - 5M kerosene-oxygen burner instead of 2 kg/s, allows steam to be emitted into the atmosphere, which greatly simplifies the system and its operation.

The average particle formation time was selected as the initial parameter for frame rate and aperture size, which was assumed to be 1/50 ÷ 1/4000 s depending on the heat load. The shooting speed is 250 ÷ 500 frames/s, the shutter speed is 1/1250 or 1/2500, and the duration of the process is up to 20 s. Granulometric composition of the peel was determined by sieve analysis.

MODEL OF A CAPILLARY-POROUS COATING

Carrying out highly heat-stressed processes is associated with the occurrence of the limiting state of a heated surface. In one case, targeted destruction of the material is carried out, for example, using rocket-type fire blast burners, from whose nozzles supersonic high-temperature flows flow, and in the other, it is necessary to create a cooling system of the nozzles and combustion chambers themselves in order to avoid a heat exchange crisis and the destruction of a steam-generating surface coated with a porous structure.

To determine the critical thermal flows and stresses, the thermoelasticity problem [2] is solved under the secondary limiting conditions for the one-dimensional equation of nonstationary heat conductivity.

Let us consider a plate with the thickness of 2h. The constant ultimate thermal flow q is supplied to the surface $z = +h$, starting from the time point $t = 0$. The bottom surface $z = -h$ and the plate side edges are thermally insulated.

Thermal conductivity equation with limiting and initial conditions can be written in the form:

$$\alpha_w \frac{\partial^2 T}{\partial z^2} = \frac{\partial T}{\partial \tau}, \quad T = 0, \quad \tau < 0;$$

$$\lambda_w \frac{\partial T}{\partial z} = q, \quad z = +h; \tag{1}$$

$$\lambda_w \frac{\partial T}{\partial z} = 0, \quad z = -h;$$

Solution to the equation (1): If we are given the limiting values of tension and compression stresses for the rock (porous coatings from the natural mineral medium) and the metal, we obtain the dependence of the thermal flow required for destruction on the time of delivery and the depth of penetration. In addition, equating the temperatures on the plate surface to the rock and metal melting temperature, we find the values of the ultimate thermal flows necessary for melting the surface layer for a different period of their action:

-surface melting:

$$q_1 = \frac{T_f}{\frac{M}{2(c\rho\lambda)_w}\tau + \frac{2}{3M} - \frac{4}{\pi^2 M}\sum_{n=1}^{\infty}\frac{(-1)^n}{n^2} exp\left[-n^2\frac{\pi^2 M^2}{4(c\rho\lambda)_w}\tau\right]\cos(n\pi)} \tag{2}$$

- creation of limiting compression stresses:

$$q_2 = \frac{\frac{(1-\nu)6_{comp.stress}}{\alpha E}}{\frac{M}{2(c\lambda\rho)_w}\tau + \frac{\frac{3z^2}{h^2}+\frac{6z}{h}-1}{12M} - \frac{4}{\pi^2 M}\sum_{n=1}^{\infty}\frac{(-1)^n}{n^2} exp\left[-n^2\frac{\pi^2 M^2}{4(c\lambda\rho)_w}\tau\right]\cos[\frac{n\pi}{2}\left(\frac{z}{h}+1\right)]} \tag{3}$$

- creation of limiting tensile stresses:

$$q_3 = \frac{\frac{(1-\nu)\sigma_{tens.stress}}{\alpha E}}{\frac{M}{2(c\lambda\rho)_w}\tau} \tag{4}$$

The functional dependences of q_1, q_2, q_3 on time for fixed values of the particle size for the coating rock, or the penetration depth of temperature disturbances for the metal, were calculated on a PC as applied to plates made of quartz, granite, tesenite, and metal. Thermo-mechanical characteristics of rock coatings and metals are summarized in Tab.1.

The wall material influences the q_{cr} value by means of the complex $(\rho c\lambda)_w$, where ρ, c, λ is the density, heat capacity and thermal conductivity of the wall respectively, but it is not appropriate to state this unambiguously, because it is practically impossible to withstand the same conditions for processing purity and microstructure.

Table 1. Thermomechanical properties of the studied material

Material	ρ, $kg/m^3\times10^3$	α, $1/K\times10^{-5}$	C, $J/(kg.K)$	λ, $W/(m.K)$	T_f, ^oC	ν	E, $N/m^2\times10^{10}$	$\sigma_{ult.tens.}$, $N/m^2\times10^6$	$\sigma_{ult.compr}$, $N/m^2\times10^6$
quartz	2,65	1,56	1172	10,8	1788	0,17	7,3	3,92	78,5
granite	2,58	1,16	921	3,15	1230	0,22	2,8	20,5	260
tesenite	2,7	5,44	937	1,44	1140	0,27	4,97	7,6	159
copper (Cu+0,56Fe)	8,9	1,6	390	390	1100	0,34	11,8	220	1570
Stainless steel 1X18H9T	7,8	1,1	516	16	1300	0,35	21,6	700	2500

When designing the combustion chamber and especially the nozzle, it is necessary to take into account a certain margin on the thickness of the heating surface. A boiling crisis will occur earlier on thin heaters, since in the pre-crisis boiling area the size of the "dry" spot at the base of the bubbles will increase, the heat transfer process will deteriorate sharply, and the wall temperature will increase. Surfaces having a large thickness will require more time to heat them up [3].

When solving the problem of thermoelasticity for the limiting state of heat transfer, the characteristic value was the thickness of detached particles (peel) δ, and when solving the same problem (heat equation (1)) for a metal surface based on the law of similar phenomena, this quantity is the penetration depth of the heat wave, which is critical in the event of a heat transfer crisis. Since the heat fluxes from the torch are destructive, in this case they also lead to the ultimate state of the enclosing elements of the burner structure (chamber and nozzle) at the time of crisis. Thus, the law of analogy allows us to use the same heat equation (1) to solve the problem of the limiting state of coatings and heat transfer surface.

ANALYTICAL STUDY

Results from the study are shown at Fig.4 and 6. The maximum thickness of the particles detaching under the action of compression forces for coatings made of quartz and granite is $(0{,}25\div0{,}3)\cdot10^{-2}$ m.

Fig.4 gives the calculation of the specific energy Q of the destruction of a granite coating volume unit. The energy Q is calculated Depending on the thickness δ of the particles being detached. The curves have pronounced minima.

The range of critical values of the specific heat fluxes in the heated layer determines the limiting and stable conduct of the cooling process at high power plant performance.

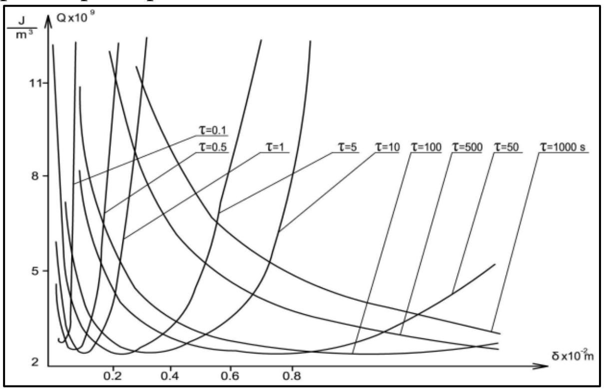

Fig.4. Change in the specific destruction energy of the granite coating Q depending on δ for different τ. $Q = q.\tau/\delta$

The upper limit of the limiting values for tensitic coating is not more than $0{,}08\cdot10^7$ W/m^2, for granite - up to $0{,}5\cdot10^7$ W/m^2, for quartz - up to 10^7 W/m^2, and the lower limit, at which particle separation is still observed under the influence of thermal stresses of compression, for quartz coating it will be $0{,}25\cdot10^7$ W/m^2, for granite five times less ($0{,}05\cdot10^7$ W/m^2), and for tensitic - respectively ten times less ($0{,}025\cdot10^7$ W/m^2). Lower specific heat fluxes will cause tensile failure of the coatings [2].

The presence of microcracks in the capillary porous system reduces the compressive strength of the coating in the vicinity of this crack so that the compressive strength can only be 2 times the tensile strength. In a continuous coating monolith, this ratio is 10 to 20 times greater.

The coating always has a fracture. Consequently, the ratio $\sigma_{lim.comp.}/\ \sigma_{lim.tens.}$ will be in the range from 2 to 10 ÷ 20.

In this regard, the specific energy consumption Q will vary within certain limits, which is well illustrated by the curves (Figs. 4-6) (similar curves are obtained for a quartz coating). Then, the previously determined limiting region q and Q for coatings of their quartz, granite, and tesenite will be between the values corresponding to the ratios $\sigma_{lim.comp.}/\sigma_{lim.tens.}$ from 2 to 10 ÷ 20.

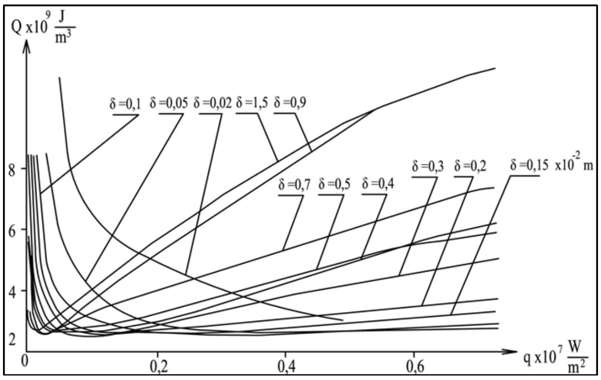

Fig.5. Change of specific destruction energy of granite coating due to q for various δ

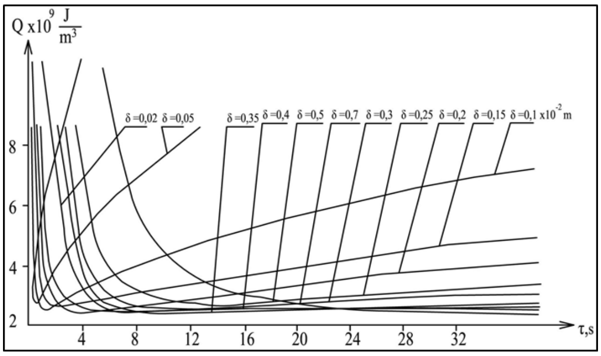

Fig.6. Change of specific destruction energy of granite coating due to τ for various δ

Since the oxygen cooler in the burners allows to develop specific heat fluxes in the stream at the main working area up to $4 \cdot 10^7$ W/m^2 and air - up to $0,6 \cdot 10^7$ W/m^2, which corresponds to specific heat fluxes in the coating of $0,74 \cdot 10^7$ W/m^2 and $0,06 \cdot 10^7$ W/m^2 - respectively, then using the proposed method, it is possible to follow the mechanism of destruction of brittle coatings from heating and to control this process.

The heated layer of rocks whilst increasing in volume, starts affecting the neigh boring less heated layers. Since extension at all other directions is blocked by reaction of non-heated layers, then rocks begin freely extend at open side and due to its overextension is getting separated and broken-off.

If cavities of vacancies could transfer to dislocation, then surface under review gets plastic properties and is not destructed under influence of flame. All metals are like that. Some rocks also have these properties. Trial was carried out with the steam generating metal surfaces of heat during the boiling crisis [1].

In terms of metals crystals are destructed under directions up to 10^{-5} V. The destruction process consists of stages of the fracture birth and their development.

Under the thermal energy impact micro fractures are born in area of stress concentrators (inclusions, discontinuity, fractures). High internal stresses also could happen due to the discontinuous process of plastic deformation, after that a fragile destruction begins. Plastic deformation is considered as the initial cause of destruction, though it can stop a growth of fractures. On one side, in centre of destruction there are ruptured links caused by heat fluctuations. On the other hand, destruction is a kinetic heat activating process which is based on transfer of vacancies towards fractures, where their growth determines destruction kinetic.

Based on the performed researches in case of irradiation by flame of the kerosene-oxygen burner of the porous coating at working area we have up to $4 \cdot 10^7$ W/m^2, which conforms to q of coating $0.4 \cdot 10^7$ W/m^2. Mechanism of the metal destruction differs crucially from mechanism of the rock destruction. Notwithstanding, based on analogy of the heat flow dependencies revealed from time of action and permeability depth of temperature perturbation that help avoid the boiling crisis in cooling system and ensure the most appropriate selection of porous coatings of minor porosity and heat conductivity. In future research of the other porous natural materials is required.

The danger of the appearance of limit thermal stresses is great at the moment of start-up and shutdown of power equipment at power plants. These stresses arise primarily in the places of concentrators, which are active vapour phase centres or condensate formation centres. The capillary-porous structure can be both of natural origin (salt deposits, tarnishes) and artificially created with well and poorly heat-conducting materials in a wide range of porosity and permeability of 3% to 90%. Structures can play a modelling role and serve as a high-intensity and forced cooling system. For example, teschenite porous coatings with a 5-fold greater lineal expansion coefficient and a 10-fold lower thermal conductivity factor and approximately the same melting point in comparison with energy steels serve as a modelling material. They are the most viscous with a porosity of up to 30%.

CONCLUSIONS

1. Using the heat balance method, functional dependencies have been established that describe the process of thermal destruction of capillary-porous coatings as a result of reaching tensile stresses or compression of limiting values, as well as in the case of surface melting.

2. It was found that for large heat fluxes and a short heating time, the compression curves are "screened" by the melting curve, and in the case of small heat fluxes and a significant time interval, by a tensile curve.

3. High-speed filming made it possible to determine the size of detached particles of capillary-porous coatings for the macroprocessing area. For example, for tesenite, their size was 2,5÷3,0 mm with a heat flux of $1{,}2{\cdot}10^6$ W/m^2; particle formation time – 2,2 s.

4. For quartz coating, the limits of destructive heat fluxes were $8{\cdot}10^4 \div 7{\cdot}10^7$ W/m^2 and for granite coating respectively $21{\cdot}10^4 \div 1{\cdot}10^7$ W/m^2.

5. The minimum fracture energy, for example, for a tense coating is $0{,}5{\cdot}10^9$ J/m^3 with a heat supply time of 0,1 ÷ 5 s and a particle size of 1 ÷ 4 mm.

6. The described approach can be useful for modelling salt deposits, assessing the possible occurrence of fatigue cracks during commissioning, as well as in calculating capillary-porous cooling systems for turbine equipment in power plants.

NOMENCLATURE

δ – thickness of the structure (depth of wave propagation, particles size), m;
λ – thermal conductivity, W/(m.K);
ν – Poisson ratio (lateral contraction);
τ – time, s;
ρ – density, kg/m^3;
σ – stress, N/m^2;
z – coordinate, m;
q – thermal load, W/m^2;
Q – specific crushing energy, J/m^3
T – temperature, K;
E – Young's modulus (elasticity modulus), Pa;
h – film height, thickness, m;
c – thermal capacity, J/(kg.K);
a – thermal diffusivity, m^2/s;
$2h$ – plate thickness, m;
Q_{cr} – heat load, W/m^2;
$\sigma_{lim.stress}$ – limited tensile stress, N/m^2;
$\sigma_{lim.compr.}$ – limited compression stress, N/m^2

REFERENCES

[1] A.A. Genbach, D. Yu. Bondartsev, I. K. Iliev, Investigation of a high-forced cooling system for the elements of heat power installations, *J. of machine Eng.* **18**, 106-117 (2018).

[2] A. A. Genbach, D. Yu. Bondartsev, I. K. Iliev, Modelling of capillary coatings and heat exchange surfaces of elements of thermal power plants, *Bulg.Chem.Comm.* **50**, 133 – 139 (2018).

[3] A. A. Genbach, D. Yu. Bondartsev, I. K. Iliev, Heat transfer crisis in the capillary-porous cooling system of elements of heat and power installations. *Thermal Science*. **23** (2A), 849-860. (2019).

[4] A. A. Genbach, K. K. Shokolakov, Development of an experimental plant of a non-nozzle porous foam generator for producing with foam generating and defoaming structures. News of the National Academy of Sciences of the Republic of Kazakhstan, *Series of Geology and Technical Sciences*, **3**, № 429, 300 – 308 (2018).

[5] E. G. Shklover, Experimental study of heat transfer from porous surface in pool and forced – convection boiling at low pressures, *Phase Change Heat Transfer ASME*, **159**, 75-80 (1991).

[6] A.S. Surtaev, V.S. Serdyukov, A.N. Pavlenko, D.V. Kozlov, D.S. Selishchev. Characteristics of boiling heat transfer on hydrophilic surface with SiO_2 coating. *Bulgarian Chemical Communications*, **50**, 36 – 44 (2018).

[7] L.L. Tovazhnyanskyy, P.O. Kapustenko, O.A. Vasilenko, S.K. Kusakov, O.P. Arsenyeva, P.Y. Arsenyev, Mathematical model of a plate heat exchanger for condensation of steam in the presence of non-condensing gas, *Bulgarian Chemical Communications*, **50**, 76 – 82, (2018).

[8] M. Jamialahmadi, H. Müller-Steinhagen, H. Abdollahi, A. Shariati, Experimental and theoretical studies on subcooled flow boiling of pure liquids and multicomponent mixtures, *Int. J. Heat and Mass Transfer*, **51**, (2008).

[9] E. Krepper, B. Koncar, Yu Egorov. CFD modelling of subcooled boiling - Concept, validation and application to fuel assembly design, *Nucl. Eng. & Design* **7**, 716-731 (2007).

[10] M. Kupetz, J. Heiew, F. Hiss, Modernization and extension of the life of steam turbine power plants in Eastern Europe and Russia, *Heat Power Engineering*, **6**, 35-43 (2014).

[11] E. A. Grin, The possibilities of fracture mechanics in relation to the problems of strength, resource and justification for the safe operation of thermal mechanical equipment, *Heat Power Engineering*, **1**, 25-32 (2014).

[12] [12] Z. Q. Yu, G. S. Zhou, S. D. Zhu, J. M. Li, L. J. Li, Influence of sensitizing treatment on the corrosion resistance of Incoloy 028 alloy. *Bulg. Chem. Comm.*, **49**, 4, 943 – 47 (2017).